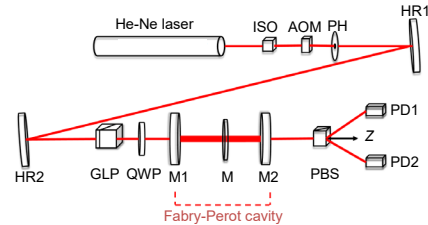


DOI: 10.12086/oe.2021.210270

偏振光腔衰荡技术测量 单层 SiO₂ 薄膜特性

武梅好, 王静*, 李斌成

电子科技大学光电科学与工程学院, 四川 成都 610054



摘要: 为了探究特定沉积工艺参数下, 不同沉积角度对 SiO₂ 光学薄膜损耗及应力双折射的影响, 本文采用一种高灵敏探测方法——偏振光腔衰荡技术表征单层 SiO₂ 光学薄膜。该技术基于测量光学谐振腔内偏振光来回反射累积后的衰荡时间特性及产生的相位差振荡频率, 实现光学元件的光学损耗和残余应力的同点、同时绝对测量。实验对 60°、70° 和 80° 沉积角度条件下制备的单层 SiO₂ 薄膜样品进行了应力和光学损耗的测量分析。结果显示了不同沉积角度条件下制备的 SiO₂ 薄膜表面粗糙程度和致密性变化对薄膜损耗和应力双折射效应的影响, 该结果对制备低光学损耗、低应力 SiO₂ 光学薄膜提供了技术指导。

关键词: 偏振光腔衰荡; 光学损耗; 应力双折射; SiO₂ 光学薄膜

中图分类号: O484.4

文献标志码: A

武梅好, 王静, 李斌成. 偏振光腔衰荡技术测量单层 SiO₂ 薄膜特性[J]. 光电工程, 2021, 48(11): 210270

Wu M Y, Wang J, Li B C. Polarized cavity ring-down technique for characterization of single-layer SiO₂ films[J]. *Opto-Electron Eng.* 2021, 48(11): 210270

Polarized cavity ring-down technique for characterization of single-layer SiO₂ films

Wu Meiyu, Wang Jing*, Li Bincheng

School of Optoelectronic Science and Engineering, University of Electronic Science and Technology of China, Chengdu, Sichuan 610054, China

Abstract: In this paper, a highly sensitive detection method - polarized cavity ring-down (P-CRD) technique - is employed to investigate the influence of deposition angle on the optical loss and stress-induced birefringence of single-layer SiO₂ films prepared with specific deposition process parameters. The P-CRD technique is based on measuring the decay behavior of accumulated polarized light reflecting back and forth inside a resonant cavity. The decay time and oscillating frequency of resulted phase difference of the CRD signal are applied to measure simultaneously the absolute values of the optical loss and residual stress-induced birefringence at the same measurement point of single-layer SiO₂ films. In the experiment, the optical losses and stress-induced birefringence of the single-layer SiO₂ film samples prepared under different deposition angles of 60°, 70°, and 80° are measured and analyzed. The results revealed the effects of the changes of surface roughness and film compact density caused by the different deposition angles on the optical loss and stress-induced birefringence of the single-layer SiO₂ films,

收稿日期: 2021-08-20; 收到修改稿日期: 2021-11-11

作者简介: 武梅好(1996-), 女, 硕士研究生, 主要从事偏振光腔衰荡技术的研究。E-mail: 201921050434@std.uestc.edu.cn

通信作者: 王静(1985-), 女, 博士, 副教授, 主要从事光学检测技术、光腔衰荡技术方面的研究。E-mail: jingwang1230@uestc.edu.cn

版权所有©2021 中国科学院光电技术研究所

respectively. These results are helpful to the preparation of high-performance SiO₂ films with low optical loss and low residual stress.

Keywords: polarized cavity ring-down; optical loss; stress induced birefringence; SiO₂ films

1 引言

随着高精密光学系统及高功率激光技术的快速发展,对光学或激光系统中光学元件的薄膜性能要求日益提高,薄膜光学损耗(包括吸收和散射损耗)是重要的性能参数之一^[1-2]。薄膜在满足超低吸收和散射损耗并能被准确测量的同时,还必须控制镀膜后的残余应力大小^[3-4]。若薄膜存在过大的残余应力,会导致基板面形弯曲、膜层破裂和脱落^[5],很大程度上限制了其光学性能,较为严重的残余应力,还会使入射到薄膜上的反射光波前产生很大的畸变,偏离光学系统路径而无法正常工作^[6]。因此对薄膜光学元件的光学损耗和应力特性的准确测量是制备低损耗、应力可控薄膜的前提。目前,针对薄膜光学元件应力无损测量技术,根据测量依据大致可以分为两类,一类是使用较为广泛的基于应力形变的测量方法^[7],如 Stoney 曲率法、X 射线衍射法(X-ray diffraction)、显微拉曼光谱法等;另一类是基于双折射效应的测量方法^[8],包括数字光弹法、光弹调制器法、偏振光腔衰荡技术等,其中偏振光腔衰荡技术通过测量谐振腔内偏振光来回反射累积产生的应力双折射振荡频率和衰荡时间,可以同时计算出光学元件的双折射相位差和光学损耗,其优势是可以实现光学元件残余应力和光学损耗的同点、同时测量,并且测量时不受光强波动的影响,具有良好

的抗噪声能力,是测量精度最高的方法^[9-13]。

光学薄膜领域中, SiO₂ 因其具有吸收率小、耐腐蚀、硬度高等特性,是制备光学薄膜的优选材料^[14-17],如在高性能光学薄膜元件和高功率激光薄膜元件中是最常用的低折射率材料,因而研究 SiO₂ 薄膜的光学损耗和应力特性显得尤为重要。相关文献^[18-21]报道的应力数据表明,薄膜特性与制备薄膜时的沉积条件密不可分。例如采用倾斜沉积技术制备薄膜时,有文献^[22-23]报道了改变沉积通量相对于基底的角度,会影响薄膜柱状微结构,进而影响薄膜的光学、力学特性。

为了探究不同沉积角度对 SiO₂ 薄膜特性的影响,本文分别对沉积角度为 60°、70°和 80°的 SiO₂ 单层膜样品的光学损耗及残余应力双折射进行了测量,并结合总积分散射仪测量的结果进行分析,得出了随沉积角度的变化以及两者的变化趋势,对膜层光学损耗和残余应力的控制提供了一定的参考价值。

2 应力、损耗测量原理

偏振光腔衰荡技术测量偏振光在谐振腔内来回反射后光腔输出的光能量衰减到原来 1/e 处所用的时间。当谐振腔内未插入被测样品时,腔长为 L_0 ,腔镜 M1、M2 反射率为 R_1 、 R_2 ,如图 1 所示,激光进入谐振腔后,光腔输出信号可表示为

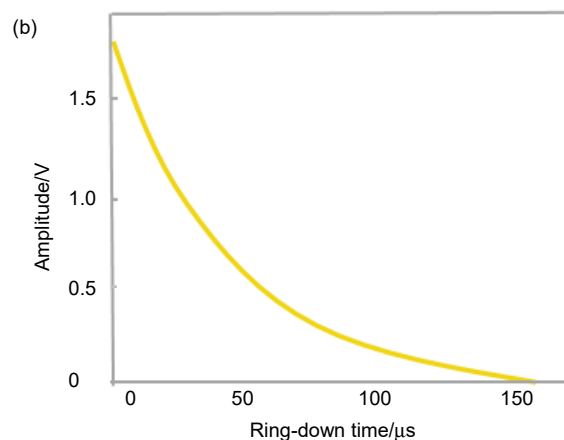
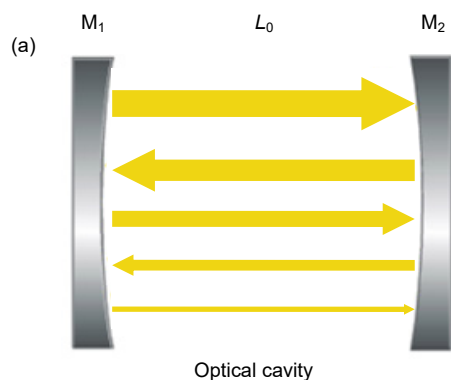


图 1 光腔衰荡技术的初始腔光路(a)及对应的衰荡曲线(b)

Fig. 1 The initial cavity configuration (a) and corresponding ring-down curve (b) for a cavity ring-down technique

$$I(t) = A \exp\left(-\frac{t}{\tau_0}\right) + B, \quad (1)$$

其中: A 表示衰荡信号的振幅, B 表示探测器直流偏置信号, τ_0 与谐振腔内的损耗(几何偏折损耗、衍射损耗、腔镜的透过、吸收和散射损耗)有关, 表示未插入待测样品时的初始腔衰荡时间:

$$\tau_0 = -\frac{L_0}{c(\ln\sqrt{R_1 R_2})}. \quad (2)$$

将待测薄膜样品垂直插入谐振腔内, 测量点处的应力双折射视为相位差 δ 、快轴角度为 θ 角的波片。光腔出射光经过沃拉斯顿分光棱镜后得到双折射衰荡信号, 如图 2 所示, 输出信号表示为

$$I(t) = A \exp\left(-\frac{t}{\tau}\right)[1 + m \sin(\omega t + \varphi)] + B, \quad (3)$$

其中: A 表示衰荡信号的振幅, τ 表示插入样品后的测试腔衰荡时间, m 表示 \sin 调制信号的系数, φ 表示振荡初始相位, ω 表示谐振拍频, B 表示探测器直流偏置信号。利用沉积角度不同的薄膜样品所对应的双折射衰荡时间 τ , 对比未插入薄膜样品的初始腔拟合得到的衰荡时间 τ_0 , 可以得到不同单层膜的光学损耗 α_{Loss} , 包括吸收和散射损耗, 表达式如下:

$$\alpha_{\text{Loss}} = 1 - \exp\left(\frac{1}{c}\left(\frac{L_0}{\tau_0} - \frac{L}{\tau}\right)\right). \quad (4)$$

另外, 根据偏振双折射衰荡信号振荡频率 ω 可以计算出被测薄膜光学元件的双折射相位差 δ 和光程差(OPD) $\Delta\sigma$:

$$\delta = \frac{L}{c} \omega = \frac{2\pi}{\lambda} \Delta\sigma, \quad (5)$$

其中: L 表示谐振腔内插入被测样品之后的腔长, c 表示真空光速, λ 为探测激光波长。

3 实验及结果分析

3.1 实验装置

偏振光腔衰荡技术(Polarized cavity ring-down, P-CRD)测量应力双折射的实验装置如图 3 所示: 633 nm 连续波 He-Ne 激光束经过光隔离器(isolator, ISO)后输出线偏振光, 通过声光调制器(acoustic optical modulator, AOM)和两个高反射镜 HR1、HR2 后输出椭圆偏振光, 旋转 Glan 偏振棱镜(Glan laser polarizer, GLP)和 1/4 波片(quarter wave plate, QWP)构成的起偏器使得输出光近似为圆偏振光, 垂直入射到由 M1、M2 构成的光学谐振腔(衰荡腔)中, 来回反射并多次通过垂直放置的待测薄膜样品 M, 由于谐振腔内光学元件 M 残余应力导致的折射率各向异性, 产生了两个具有不同纵模频率 ω_1 、 ω_2 的正交偏振模式, 当谐振腔内能量累积超过提前所设定的阈值时, 声光调制器关断激光, 光学谐振腔输出光通过透光轴在 x 、 y 轴上的偏振分光棱镜(polarized beamsplitter, PBS)后分成两束偏振方向相互正交、能量变化此起彼伏的线偏振光, 分别是 S 光和 P 光, 利用数据采集卡采集光电探测器 PD1 和 PD2 探测的两束线偏振光的光电信号, 得到的光腔衰荡信号偏离单指数形式进行振荡衰荡, 振荡频率 ω 与两个正交模式的干涉拍频有关($\omega = \omega_1 - \omega_2$), 其腔内双折射相位差 δ 、光程差(optical path difference, OPD)满足线性关系如式(5)。

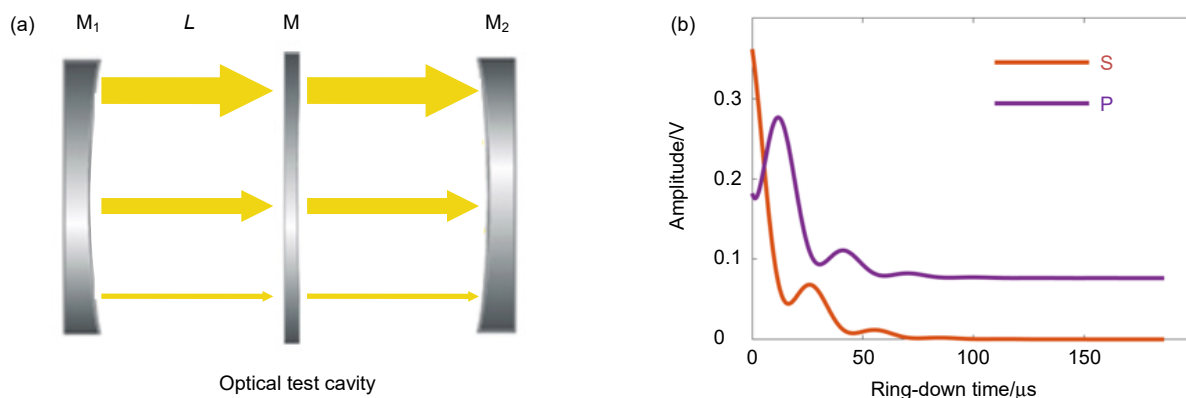


图 2 测试腔光路(a)及对应的振荡衰荡曲线(b)

Fig. 2 Test cavity configuration (a) and the corresponding oscillation ring-down curve (b)

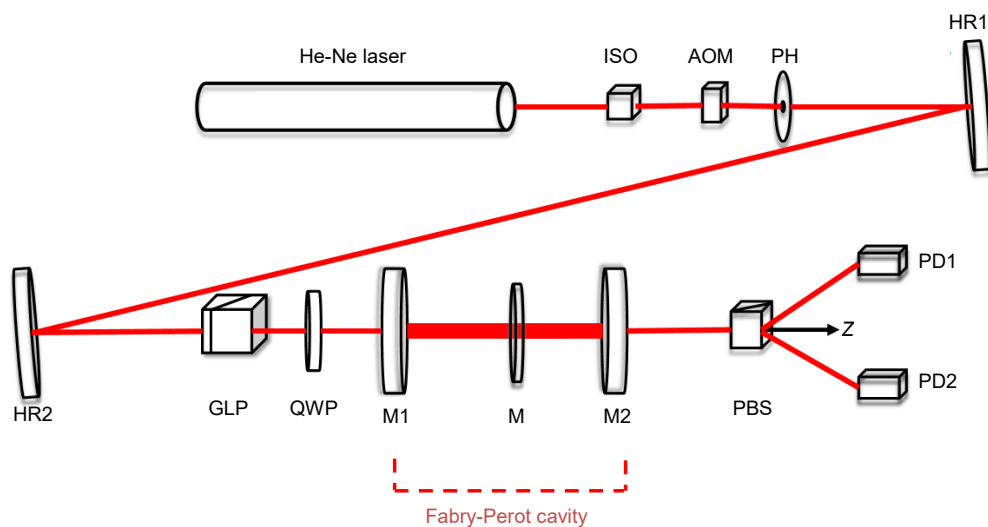


图3 偏振光腔衰荡技术测量光学元件光学损耗和应力双折射实验装置。
 ISO: 光隔离器; AOM: 声光调制器; PH: 小孔光阑; HR1、HR2: 高反射镜 R_1 、 R_2 ;
 GLP: Glan 偏振棱镜; QWP: 1/4 波片; M1、M2: 谐振腔镜; M: 待测光学元件;
 PBS: 偏振分光棱镜; PD1、PD2: 光电探测器 1、2; Z: 光传播方向

Fig. 3 Experimental arrangement of polarized cavity ring-down to measure the optical loss and stress-induced birefringence of optical components.

ISO: optical isolator; AOM: acousto-optic modulator; PH: small aperture diaphragm; HR1, HR2: high reflector R_1 , R_2 ; GLP: Glan polarizing prism; QWP: 1/4 wave plate; M1, M2: resonator mirror; M: optical component to be tested; PBS: polarization beam splitter prism; PD1, PD2: photodetector 1, 2; Z: light propagation direction

3.2 测量结果

基于上述实验装置和衰荡信号拟合公式, 对特定沉积工艺参数下(沉积速率 1.6 A/S), 采用离子束溅射 (ion beam sputtering, IBS) 技术^[24]和 SiO_2 靶材(纯度 99.99%)制备沉积角度分别为 60° 、 70° 、 80° , 直径 25.4 mm 的 SiO_2 单层膜样品进行测量。其中, 沉积角度 θ 是指镀膜基片所在的斜面与水平方向的倾斜角度(假

设离子束垂直溅射), 如图 4 所示, 制备薄膜时将基底固定在加装好的倾斜柱的斜面上, 使溅射沉积通量与基底表面呈不同的角度, 从而获得不同沉积角度的 SiO_2 单层膜。利用分光光度计测试样品透过率、反射率光谱, 通过 Optilayer 软件拟合光谱曲线获得薄膜厚度。表 1 所示是不同沉积角度的单层膜样品对应的薄膜厚度。

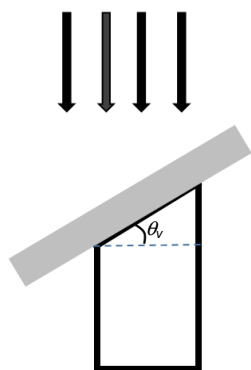


图4 倾斜沉积技术制备单层膜样品

Fig. 4 Oblique deposition technique to prepare single-layer film samples

表1 不同沉积角度的待测单层膜样品对应的薄膜厚度

Table 1 The film thickness corresponding to the single-layer film samples with different deposition angles

Deposition angle/($^\circ$)	60	70	80
Film thickness/nm	170	148	137

在插入待测单层膜样品前后, 谐振腔腔长 L_0 、 L 分别是 0.531 m 和 0.533 m, 初始腔衰荡时间 τ_0 为 37.51 μs 。对三块待测单层膜样品上的一点进行重复多次测量, 根据拟合得到的测试腔衰荡时间 τ 和应力双折射振荡频率 ω , 利用式(4)、式(5), 得到不同单层膜样品的损耗和应力双折射相位差, 如图 5、图 6 所示。其中, 每次拟合是十次衰荡信号的平均, 可以看出高斯函数拟合可以很好地描述统计分布的结果。

所测得的损耗测量精度均在 ppm 量级, 其中, 沉积角度 60° 的单层膜损耗拟合平均值 22.9 ppm, 统计标准差 2.2 ppm, 沉积角度 70° 的单层膜损耗拟合平均值 36.4 ppm, 统计标准差 2.1 ppm, 沉积角度 80° 的单层膜损耗拟合平均值 52.7 ppm, 统计标准差 3.5 ppm。与传统的各种损耗分别测量(采用不同测量仪器分别对吸收、散射损耗进行测量, 最后叠加计算得到总损耗)相比, 该技术测量效率高且不存在测量点偏差, 因而可以很好地对测量点进行评估。

需要指出的是, 虽然上述测量得到的应力双折射相位差是腔内所有双折射相位差的叠加, 包括腔镜多层膜的残余应力等, 但由于实验装置空腔测量结果比测试腔双折射相位差小一个数量级, 因此, 空腔双折射值不影响待测样品测量精度, 认为上述结果可以很好地描述待测薄膜样品残余应力双折射的大小:

沉积角度 60° 的单层膜应力双折射相位差拟合平均值 6.0×10^{-4} rad(OPD 0.0607 nm), 统计标准差 5.7×10^{-6} rad(OPD 7.6×10^{-4} nm);

沉积角度 70° 的单层膜应力双折射相位差拟合平均值 4.4×10^{-4} rad(OPD 0.0441 nm), 统计标准差 7.2×10^{-6} rad(OPD 7.2×10^{-4} nm);

沉积角度 80° 的单层膜应力双折射相位差拟合平均值 2.8×10^{-4} rad(OPD 0.0284 nm), 统计标准差 5.0×10^{-6} rad(OPD 5.1×10^{-4} nm), 与光弹调制器法(相位差测量精度 5×10^{-5} rad)相比^[25], 偏振光腔衰荡法重复性测量精度提高了一个数量级, 测量准确性更高。

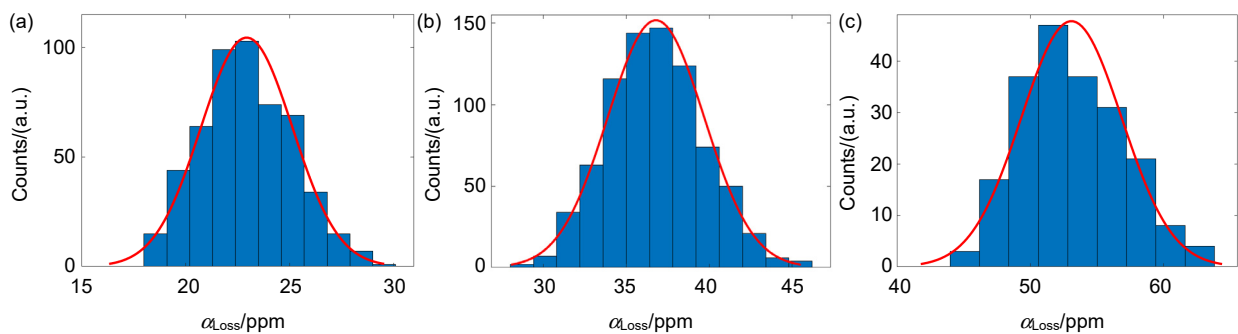


图 5 不同沉积角度制备的单层膜样品光学损耗统计分布及对应高斯拟合。(a) 60° ; (b) 70° ; (c) 80°

Fig. 5 Optical loss statistical distribution and corresponding Gaussian fitting of single-layer film samples prepared at different deposition angles. (a) 60° ; (b) 70° ; (c) 80°

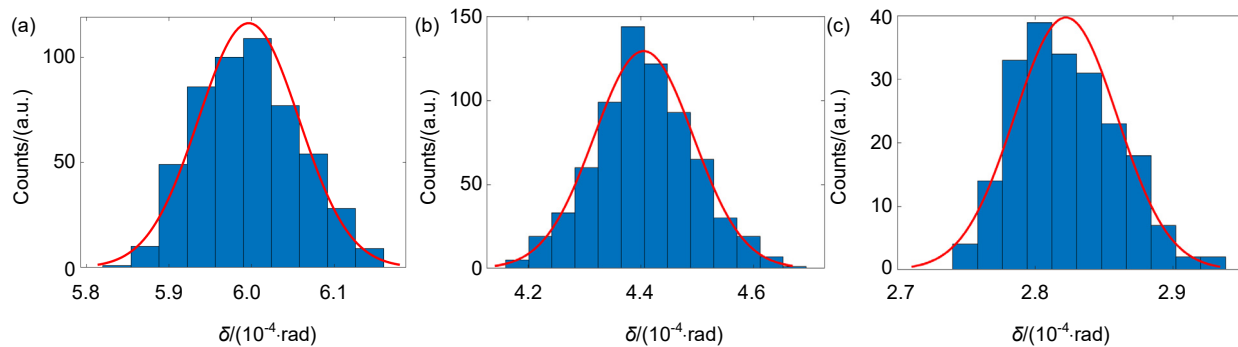


图 6 不同沉积角度制备的单层膜样品应力双折射相位差统计分布及对应高斯拟合。(a) 60° ; (b) 70° ; (c) 80°

Fig. 6 Statistical distribution of stress birefringence phase difference and corresponding Gaussian fitting of single-layer film samples prepared at different deposition angles. (a) 60° ; (b) 70° ; (c) 80°

表 2 不同沉积角度单层膜样品损耗、残余应力测量结果

Table 2 Measurement results of optical loss and residual stress of single-layer film samples at different deposition angles

Deposition angle/(°)	60	70	80
$\alpha_{\text{Loss}}/\text{ppm}$	22.9±2.2	36.4±2.1	52.7±3.5
$\delta/(10^{-4}\cdot\text{rad})$	5.987±0.057	4.379±0.072	2.796±0.05

3.3 分析和讨论

相关文献^[26-27]表明, 在溅射沉积初期薄膜形貌近似为孤立的岛状结构, 随着膜厚的增加, 晶粒度和岛状结构不断增加, 散射随之增大。但当膜厚增加到一定程度后, 岛之间相互结合形成走向随机的通道, 进而生长成网状结构, 使得散射迅速减少。随着膜厚进一步增加(>100 nm), 在薄膜生长后期薄膜形貌进入连续膜阶段, 单位体积内晶界随着晶粒度的增加逐渐减少, 进而对光的表面散射随之减少并逐渐趋于一个稳定值。因而, 对于 SiO₂连续薄膜材料来说, 膜层厚度对表面散射的影响可忽略不计, 对此仅考虑沉积角度对表面散射的影响。

同时使用总积分散射(total integrated scattering, TIS)仪器测量了单层膜散射随沉积角度的变化规律, 测量结果如表 3 所示。沉积角度 60°、70°和 80°的单层膜前、后散射之和分别为 45.8 ppm、84.7 ppm 和 100 ppm。可以看出, 随着沉积角度的增大, 散射损耗呈逐渐增大的趋势。根据表面微粗糙度(root mean square, RMS)和表面散射之间的关系^[28-30], 总积分散射主要受 RMS 粗糙度的影响, 上述测量结果表明, 随着沉积角度的增加, 单层膜表面 RMS 粗糙度增大, 造成表面散射增强, 光学损耗增加。

需要说明的是, 由于薄膜存在一定的非均匀性, 并且 TIS 仪器由于标定误差、测量点偏差等因素, 测量的散射损耗明显高于基于光腔衰荡技术测量的总光学损耗(近似为 2 倍关系), 但两者测量结果的趋势非常一致。根据总积分散射的定义:

$$\frac{P}{R_0 P_0 + P}$$

其中: P 是散射光能量, R_0 是镜面反射率, P_0 是入射光能量。

测量结果显示: 被测元件的光学损耗主要为散射损耗, 吸收损耗相对较低。由于光腔衰荡技术为绝对测量技术, 不需要标定, 且不存在测量点偏差, 可以认为采用偏振光腔衰荡技术测量的高透薄膜光学元件的光学损耗更准确。

图 7 所示为不同沉积角度的 SiO₂ 单层膜样品的光学损耗 α_{Loss} 及双折射相位差 δ 的测量结果。可以看出, 随着沉积角度增加, 单层膜损耗呈逐渐递增的趋势, 这主要是因为, 随着沉积角度的增加, 溅射沉积入射原子沿基片表面迁移速率增大。在沉积初期, 不同沉积角对应的晶粒生长并没有明显区别。但随着晶粒不断生长, 入射原子只能在突出的晶粒上凝结分布, 而突出周围区域形成了阴影区, 入射原子不能直接到达,

表 3 待测不同沉积角度的单层膜样品的散射测量结果

Table 3 Scattering measurement results of single-layer film samples with different deposition angles to be measured

Angle/(°)	60	70	80
Back scatter			
Mean/ppm	19.1	28.2	50.3
Angle/(°)	60	70	80
Forward scatter			
Mean/ppm	26.7	56.5	49.7

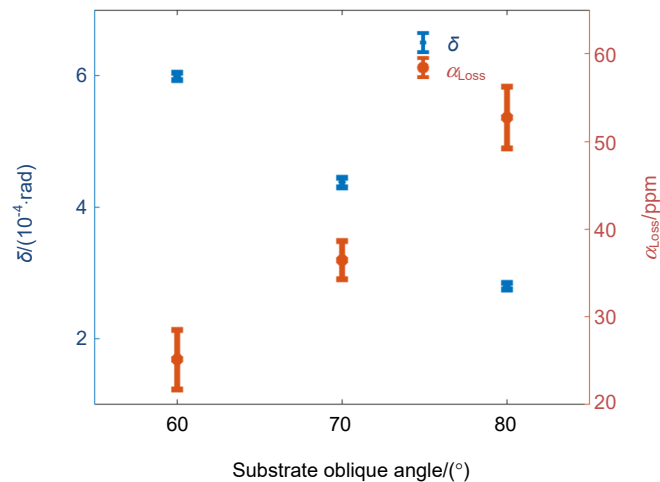


图7 沉积角度对单层膜光学损耗、残余应力影响

Fig. 7 The influence of deposition angle on optical loss and residual stress of single-layer film samples

只能通过沿面迁移到达,晶粒便逐渐向入射原子的沉积方向倾斜生长,薄膜逐渐变得粗糙。此过程与总积分散射测量的结果保持一致:沉积角度会影响 SiO_2 薄膜表面的粗糙程度,进而影响其损耗大小。而单层膜残余应力导致的相位差随着沉积角度的增大,呈逐渐减小的趋势,是因为随着沉积角度、表面粗糙程度的增加,薄膜越倾向于疏松多孔的结构。文献[31]表明,残余应力大小与薄膜密度存在较强的相关性,薄膜致密性越疏松,对应的应力逐渐减小,使得测量得到的应力双折射相位差随之逐渐减小。

4 结论

本文采用的偏振光腔衰荡技术,将应力双折射测量转为对振荡频率的测量,同时将损耗测量转为对衰荡时间的测量,可以实现薄膜光学元件光学损耗和应力的同点、同时测量。实验对不同沉积角度的 SiO_2 单层膜样品光学损耗和应力特性进行了测量。分析表明,随着沉积角度增加,薄膜粗糙度增大,致密性越来越疏松。对应地,薄膜光学损耗呈逐渐增大的趋势,应力双折射呈逐渐减小的趋势,这一趋势与总积分散射测量元件表面微粗糙度具有一致性。该实验装置的应力双折射重复性测量精度可达 5.0×10^{-6} rad,损耗测量精度达到 ppm 量级,证实了偏振光腔衰荡技术较目前使用的光弹调制器法具有更高的测量精度,可以很好地应用在薄膜光学特性参数测量中,具有广阔的应用前景。

致谢

本文工作得到了同济大学张锦龙老师的帮助,感谢张老师提供的三块不同沉积角度的 SiO_2 单层膜样品。

参考文献

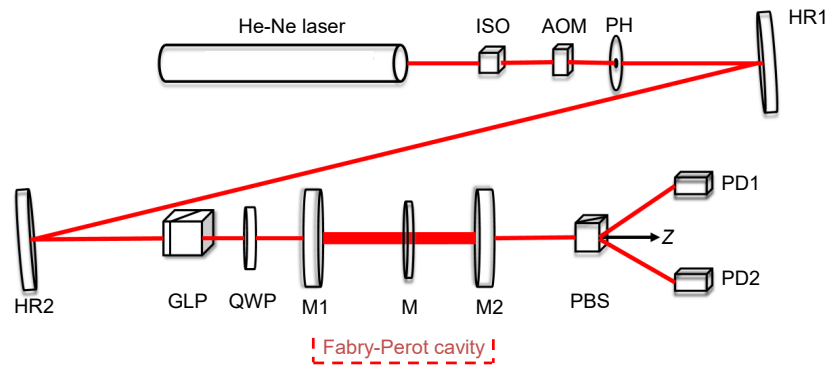
- [1] Fang Z X. Losses of optical thin films[J]. *Chin J Lasers*, 1981, **8**(8): 45–53.
范正修. 光学薄膜的损耗[J]. 中国激光, 1981, **8**(8): 45–53.
- [2] Jing J H, Kong M D, Wang Q, et al. Measurement of absorption loss of optical thin-film by infrared thermal imaging[J]. *Opto-Electron Eng*, 2021, **48**(6): 210071.
荆建行, 孔明东, 王强, 等. 基于红外热像仪的光学薄膜吸收测试方法[J]. 光电工程, 2021, **48**(6): 210071.
- [3] Dahmani F, Schmid A W, Lambropoulos J C, et al. Dependence of birefringence and residual stress near laser-induced cracks in fused silica on laser fluence and on laser-pulse number[J]. *Appl Opt*, 1998, **37**(33): 7772–7784.
- [4] Shao S Y, Fan Z X, Fan R Y, et al. Study of residual stress in ZrO_2 thin films[J]. *Acta Opt Sin*, 2004, **24**(4): 437–441.
邵淑英, 范正修, 范瑞瑛, 等. ZrO_2 薄膜残余应力实验研究[J]. 光学学报, 2004, **24**(4): 437–441.
- [5] Shao S Y, Fan Z X, Fan R Y, et al. A review of study of stress in thin films[J]. *Laser Optoelectron Prog*, 2005, **42**(1): 22–27.
邵淑英, 范正修, 范瑞瑛, 等. 薄膜应力研究[J]. 激光与光电子学进展, 2005, **42**(1): 22–27.
- [6] Stout J H, Shores D A, Goedjen J G, et al. Stresses and cracking of oxide scales[J]. *Mater Sci Eng A*, 1989, **120–121**: 193–197.
- [7] Sethuraman V A, Chon M J, Shimshak M, et al. In situ measurements of stress evolution in silicon thin films during electrochemical lithiation and delithiation[J]. *J Power Sources*, 2010, **195**(15): 5062–5066.

- [8] Xiao S L, Li B C. Residual stress measurement methods of optics[J]. *Opto-Electron Eng*, 2020, **47**(8): 190068.
肖石磊, 李斌成. 光学元件残余应力无损检测技术概述[J]. *光电工程*, 2020, **47**(8): 190068.
- [9] Xiao S L, Li B C, Cui H, et al. Sensitive measurement of stress birefringence of fused silica substrates with cavity ring-down technique[J]. *Opt Lett*, 2018, **43**(4): 843–846.
- [10] Huang H F, Lehmann K K. Effects of linear birefringence and polarization-dependent loss of supermirrors in cavity ring-down spectroscopy[J]. *Appl Opt*, 2008, **47**(21): 3817–3827.
- [11] Dupré P. Birefringence-induced frequency beating in high-finesse cavities by continuous-wave cavity ring-down spectroscopy[J]. *Phys Rev A*, 2015, **92**(5): 053817.
- [12] Fleisher A J, Long D A, Liu Q N, et al. Precision interferometric measurements of mirror birefringence in high-finesse optical resonators[J]. *Phys Rev A*, 2016, **93**(1): 013833.
- [13] Visschers J C, Tretiak O, Budker D, et al. continuous-wave cavity ring-down polarimetry[J]. *J Chem Phys*, 2020, **152**(16): 164202.
- [14] Atanassova E, Dimitrova T, Koprinarova J. AES and XPS study of thin RF-sputtered Ta₂O₅ layers[J]. *Appl Surf Sci*, 1995, **84**(2): 193–202.
- [15] Neaton J B, Muller D A, Ashcroft N W. Electronic properties of the Si/SiO₂ interface from first principles[J]. *Phys Rev Lett*, 2000, **85**(6): 1298–1301.
- [16] Tomozeiu N. SiO_x thin films deposited by r.f. magnetron reactive sputtering: structural properties designed by deposition conditions[J]. *J Optoelectron Adv Mater*, 2006, **8**(2): 769–775.
- [17] Kong M D, Li B C, Guo C, et al. Characteristics of absorption edge of SiO₂ films[J]. *Opto-Electron Eng*, 2019, **46**(4): 180220.
孔明东, 李斌成, 郭春, 等. SiO₂ 光学薄膜的吸收边特性[J]. *光电工程*, 2019, **46**(4): 180220.
- [18] Zheng M J, Zhang L D, Liu F M. Preparation and optical properties of SiO₂ thin films containing InP nanocrystals[J]. *Mater Res Bull*, 2000, **35**(14–15): 2469–2477.
- [19] Shintani A, Sugaki S, Nakashima H. Temperature dependence of stresses in chemical vapor deposited vitreous films[J]. *J Appl Phys*, 1980, **51**(8): 4197–4205.
- [20] Revesz A G, Hughes H L. The structural aspects of non-crystalline SiO₂ films on silicon: a review[J]. *J Non Cryst Solids*, 2003, **328**(1–3): 48–63.
- [21] Lin D W, Huang W, Xiong S M, et al. Effect of different deposition angle on the performance of YbF₃ film[J]. *Opto-Electron Eng*, 2011, **38**(1): 103–106.
林大伟, 黄伟, 熊胜明, 等. 不同沉积角度对氟化镱薄膜性质的影响[J]. *光电工程*, 2011, **38**(1): 103–106.
- [22] Kupfer H, Flügel T, Richter F, et al. Intrinsic stress in dielectric thin films for micromechanical components[J]. *Surf Coat Technol*, 1999, **116–119**: 116–120.
- [23] Choi J K, Lee J, Yoo J B, et al. Residual stress analysis of SiO₂ films deposited by plasma-enhanced chemical vapor deposition[J]. *Surf Coat Technol*, 2000, **131**(1–3): 153–157.
- [24] Wang Y Z, Gong G Q, Cui J Z. Preparation and application of SiO₂ thin films[J]. *Vacuum Cryog*, 2003, **9**(4): 228–233.
王永珍, 龚国权, 崔敬忠. 二氧化硅薄膜的制备及应用[J]. *真空与低温*, 2003, **9**(4): 228–233.
- [25] Wang B L, Oakberg T C. A new instrument for measuring both the magnitude and angle of low level linear birefringence[J]. *Rev Sci Instrum*, 1999, **70**(10): 3847–3854.
- [26] Fang M, Hu D F, Shao J D. Evolution of stress in evaporated silicon dioxide thin films[J]. *Chin Opt Lett*, 2010, **8**(1): 119–122.
- [27] Zhang Y D, Liu H X. Production of optical coatings with ion beam sputter deposition technique[J]. *Opto-Electron Eng*, 2001, **28**(5): 69–72.
张云洞, 刘洪祥. 离子束溅射沉积干涉光学薄膜技术[J]. *光电工程*, 2001, **28**(5): 69–72.
- [28] Amra C, Roche P, Pelletier E. Interface roughness cross-correlation laws deduced from scattering diagram measurements on optical multilayers: effect of the material grain size[J]. *J Opt Soc Am B*, 1987, **4**(7): 1087–1093.
- [29] Hou H H, Sun X L, Shen Y M, et al. Roughness and light scattering properties of ZrO₂ thin films deposited by electron beam evaporation[J]. *Acta Phys Sin*, 2006, **55**(6): 3124–3127.
侯海虹, 孙喜莲, 申雁鸣, 等. 电子束蒸发氧化锆薄膜的粗糙度和光散射特性[J]. *物理学报*, 2006, **55**(6): 3124–3127.
- [30] Hou H H, Sun X L, Tian G L, et al. Research on the surface scattering properties of optical films by the total integrated scatter[J]. *Acta Phys Sin*, 2009, **58**(9): 6425–6429.
侯海虹, 孙喜莲, 田光磊, 等. 利用总积分散射仪对光学薄膜表面散射特性的研究[J]. *物理学报*, 2009, **58**(9): 6425–6429.
- [31] Gu P F. *Technology of Thin Film*[M]. Hangzhou: Zhejiang University Press, 1990: 80–81.
顾培夫. *薄膜技术*[M]. 杭州: 浙江大学出版社, 1990: 80–81.

Polarized cavity ring-down technique for characterization of single-layer SiO₂ films

Wu Meiyu, Wang Jing*, Li Bincheng

School of Optoelectronic Science and Engineering, University of Electronic Science and Technology of China, Chengdu, Sichuan 610054, China



Experimental arrangement of polarized cavity ring-down to measure the optical loss and stress induced birefringence of optical components

Overview: Silicon dioxide (SiO₂) is a preferred low index of refraction material for preparing high-performance optical films because of its low absorption coefficient, high corrosion resistance, high hardness, and so on. During the preparation of optical thin films, the residual stress inside the films needs to be well controlled; otherwise, it may cause surface deformation and refractive index anisotropy of corresponding optical components. There are many methods for measuring residual stress inside optical components that have limited measurement accuracy, such as the Stoney curvature method, X-ray diffraction (XRD) method, photoelastic modulator (PEM) method, and so on. In this paper, the stress birefringence measurement method based on polarized cavity ring-down (P-CRD) is adopted to measure simultaneously the residual stress-induced birefringence and optical loss of single-layer SiO₂ film samples. In P-CRD, the measurement of stress birefringence and optical loss is not affected by the fluctuation of light intensity as instead a delay time is measured. The measurement accuracy of the stress birefringence is significantly improved due to the cumulative effect of the polarization phase difference by multiple back and forth reflections inside the ring-down cavity. In order to explore the influence of deposition angle on the optical loss and stress birefringence of single-layer SiO₂ film samples prepared with Ion-Beam Sputtering (IBS) coating technique, three single-layer SiO₂ film samples with deposition angles of 60°, 70° and 80° were measured with P-CRD. The achieved measurement precisions were less than 3.5 ppm for the optical loss and 5.0×10^{-6} rad for the stress refringence. The measured optical losses were 22.9 ppm, 36.4 ppm, and 52.7 ppm, and the stress birefringence were 5.99×10^{-4} rad, 4.38×10^{-4} rad, and 2.80×10^{-4} rad for the samples prepared with deposition angles of 60°, 70°, and 80°, respectively. Clearly, as the deposition angle increases, the optical loss increases and the stress birefringence decreases.

The scattering losses of the single-layer SiO₂ film samples were also measured with a Total Integrated Scattering (TIS) instrument. The scattering measurement results showed that as the deposition angle increases, the surface roughness of the single-layer SiO₂ film gradually increases, resulting in increased surface scattering, which in turn increases the optical loss measured by P-CRD. In addition, the increase in surface roughness makes the film more prone to a loose and porous structure. Since the residual stress has a strong correlation with the packing density of the film, a loose structure indicates a reduced packing density, which causes the residual stress (and the stress-induced birefringence) of the film sample to decrease gradually with the increasing deposition angle.

These results not only confirmed that the polarization cavity ring-down technique has higher stress birefringence measurement accuracy than the currently most sensitive instrument based on PEM (with phase difference measurement accuracy of 5×10^{-5} rad), but also were helpful to the preparation of high-performance SiO₂ films with low optical loss and low residual stress.

Wu M Y, Wang J, Li B C. Polarized cavity ring-down technique for characterization of single-layer SiO₂ films[J]. *Opto-Electron Eng*, 2021, 48(11): 210270; DOI: 10.12086/oe.2021.210270

* E-mail: jingwang1230@uestc.edu.cn